Oral Diseases (2007) 13, 530–537. doi:10.1111/j.1601-0825.2006.01337.x

http://www.blackwellmunksgaard.com

REVIEW ARTICLE

The miniature pig: a useful large animal model for dental and orofacial research

S Wang[1], Y Liu[1], D Fang[1], S Shi[2]

[1]*Salivary Gland Disease Center and Molecular Laboratory for Gene Therapy, Capital Medical University School of Stomatology, Beijing, China;* [2]*Center for Craniofacial Molecular Biology, University of Southern California School of Dentistry, Los Angeles, CA, USA*

Compared with small animal models such as rodents, large animal models are superior in many aspects for the study of human diseases and pre-clinical therapies. Since the development of the Minnesota miniature pig in 1949 at the Hormel Institute (USA), miniature pigs have been used as a large animal model in medical studies for scientific, economic, and ethical reasons. The oral maxillofacial region of miniature pigs is similar to that of humans in anatomy, development, physiology, pathophysiology, and disease occurrence. In this review, we describe the anatomical characteristics of the oral maxillofacial system of the miniature pig, established models of oral diseases in this animal, and other uses of the miniature pig in orofacial research.

Oral Diseases (2007) **13**, 530–537

Keywords: miniature pig; laboratory animal model; oral maxillofacial region; oral diseases

Introduction

Since the development of the Minnesota miniature pig (or 'minipig') in 1949 at the Hormel Institute (USA) (England *et al*, 1954), miniature pigs have been extensively used as a large animal model in many biomedical experiments (Polejaeva *et al*, 2000; Screaton *et al*, 2003) and studies of artificial organs (Van Dorp *et al*, 1998; Xu *et al*, 2003). Among the reasons for their common use are similarities in gross anatomy and physiology to humans, as well as for economic advantages and ethical reasons. Many different types of miniature pigs have been bred and some of them spontaneously develop diseases seen in humans, involving similar processes, such as diabetes (Larsen and Rolin, 2004) or melanoma (Millikan *et al*, 1974). We have experience using miniature pigs from the Chinese Agricultural University of Beijing for oral disease studies. This kind of miniature pig, called the Chinese experimental miniature pig, was derived from little swine from Guizhou Province, China, in 1985, and its genetic background is well understood. Its characteristics include inherent small size, early sexual maturity, rapid breeding, and ease of management (Yu *et al*, 2003). In this review, we discuss applications of this miniature pig in orofacial research.

Correspondence: Dr S Wang, Salivary Gland Disease Center and Molecular Laboratory for Gene Therapy, Capital Medical University School of Stomatology, Tian Tan Xi Li No.4, Beijing 100050, China. Tel/Fax: 86 10 67062012, E-mail: songlinwang@dentist.org.cn
Received 15 August 2006; revised 11 September 2006; accepted 14 September 2006

Salivary gland research

Structure and salivary flow rate

Rodent models are widely used for salivary gland research, as the structure, function, and biology of these animals' salivary glands are relatively well understood. However, the small volumes of their salivary glands, slim diameters of the gland ducts, and the short lifespans of rodents hinder many investigators in using these animals for studies of disease mechanism. As shown in Table 1, we compared anatomical features of the miniature pig with those of other experimental animals. The results suggest that the miniature pig shares many characteristics with humans including ductal system and gland structure (Table 1, Figure 1) (Wang *et al*, 1998; Ma, 2002; Zhang *et al*, 2005). The parotid and mixed saliva flow rates in miniature pigs and humans showed no significant differences and were much higher than those in rats (Xia *et al*, 2003a; Shan *et al*, 2005). The salivary pH in both miniature pigs and rats was higher than in humans (Table 2). The acinar cells of the terminal portion of the miniature pig's parotid gland were typical serous cells (Figure 2a), and the submandibular glands were characterized by a parenchyma of mixed acini and serous acini (Figure 2b). Each lobule was structured with an intercalated duct system, and a highly prismatic epithelial lining was found in the main duct and intercalated duct. Moreover, no alcian blue positive staining was found in the parotid glands

Table 1 Anatomic comparison of salivary glands among human and five animal models

Genus	*Body weight*	*Gland*	*Gland weight (g)*		*Main duct*	
			Range	*Mean ± s.d.*	*Length (mm)*	*Diameter (mm)*
Human	60 kg	Parotid gland	15–30		50–70	2–3
		Submandibular gland	7–15		50	1–2
Miniature pig	29–42 kg	Parotid gland ($n = 22$)	10.2–20.6	14.40 ± 2.80	111–152	1–3
		Submandibular gland ($n = 10$)	8–11.5	9.10 ± 1.20	105–140	2–3
Macaque	6–8 kg	Parotid gland ($n = 3$)	11.2–15.1	13.60 ± 2.10	40–50	~2
		Submandibular gland ($n = 3$)	2.6–3.6	3.00 ± 0.53	40–50	~1
Rabbit	2.3–3.8 kg	Parotid gland ($n = 10$)	0.98–1.68	1.33 ± 0.29	40–50	~1
		Submandibular gland ($n = 10$)	0.40–0.70	0.58 ± 0.09	40–50	~0.8
Rat	290–352 g	Parotid gland ($n = 10$)	0.16–0.31	0.25 ± 0.05	25–30	~0.7
		Submandibular gland ($n = 10$)	0.20–0.28	0.24 ± 0.03	~15	~0.7
Mouse	26–46 g	Parotid gland ($n = 10$)	0.05–0.14	0.10 ± 0.03	~15	~0.5
		Submandibular gland ($n = 10$)	0.06–0.12	0.09 ± 0.03	~10	~0.5

n is the number of animals used to calculate the glands weights and characteristics of the ducts. This table summarizes data previously reported in Wang *et al* (1998), Ma (2002), and Zhang *et al* (2003, 2005).

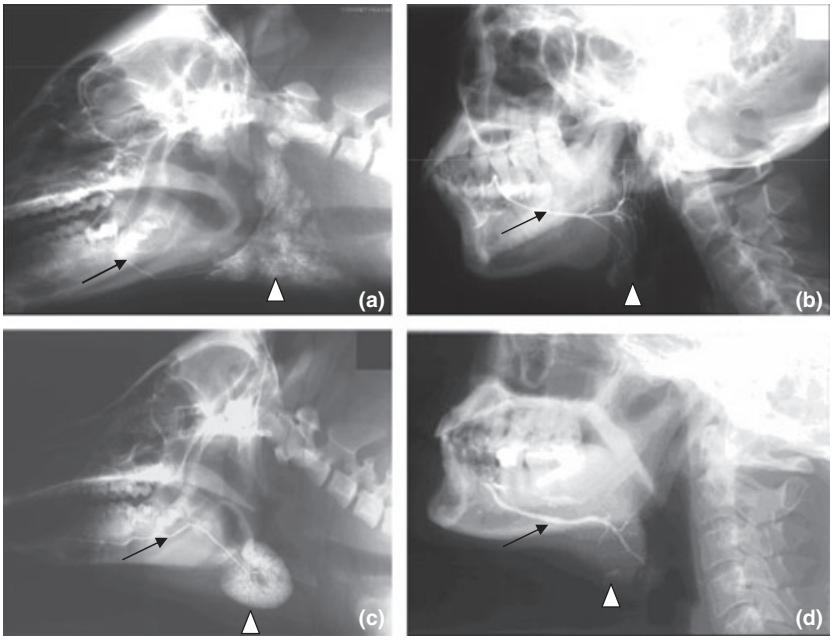

Figure 1 Miniature pig and human salivary sialograms. (**a**) Lateral sialogram of miniature pig parotid gland showing main duct (arrow), branch ducts, and triangular parotid gland (arrowhead pointing to base of triangle). (**b**) Lateral view of human parotid gland showing similar ductal system and gland structure, but smaller size of parotid gland. (**c**) Lateral view of a sialogram of a normal miniature pig submandibular gland showing a long main excretory duct (arrow) and a pear-shaped gland (arrowhead). The main duct runs horizontally along the floor of the mouth backward to the ramus mandible, turns down with a 120° angle, and then divides into two to four branches. Submandibular gland looks like an upside down pear located inferior–posterior to the angle of mandible. The margin of the miniature pig's submandibular gland is very sharp. (**d**) Lateral sialogram of human submandibular gland showing similar ductal system and gland structure

because of the absence of mucous acini (Figure 2c,d), while strong, positive alcian blue and periodic acid-Schiff staining was revealed in the mucous cells of the submandibular glands (Figure 2e,f). In general, it seems reasonable to believe that miniature pigs may a valuable animal model for salivary gland research.

Irradiation damage model of parotid gland

Salivary glands of most head and neck cancer patients often suffer irreversible damage from ionizing radiation treatment (Gosselin and Pavilonis, 2002). Rodent salivary glands are relatively radioresistant compared with human glands, perhaps due to structural differences from humans (Nagler, 2003). Many studies have suggested that the observed radiation-induced structural and functional salivary gland changes in miniature pig are comparable to those observed following irradiation of human salivary glands. When Hanford miniature pigs were subjected to a fractionated daily irradiation with a total dose of 70 Gy, the irradiated submandibular and parotid glands were one-third to one-half the gross size of control glands and showed significant parenchymal loss, with extensive acinar atrophy and interstitial fibrosis, enlarged nuclei in remaining acinar cells, and ductal dilatation and proliferation. Furthermore, stimulated salivary flow was reduced by 81% in irradiated animals compared with pre-irradiation values (Radfar and Sirois, 2003).

Our group applied a single dose of 15 or 20 Gy to miniature pigs, using a three-dimensional treatment plan system (Li *et al*, 2005b). A single dose of 20 Gy is roughly comparable to a total clinical irradiation (IR) dose of 60–65 Gy (2 Gy fractions; thrice/week), which is a calculated biologically effective dose of fractionated

Table 2 A comparison of saliva flow rates and pH in human, miniature pig, and rat

Genus	*Saliva flow rate (ml min^{-1})*		*pH*
	Parotid saliva	*Mixed saliva*	
Human	0.35 ± 0.21 ($n = 29$)	1.13 ± 0.87 ($n = 16$)	7.32 ± 0.17 ($n = 16$)
Miniature pig	0.31 ± 0.38 ($n = 18$)	1.40 ± 0.39 ($n = 12$)	7.77 ± 0.18* ($n = 12$)
Rat		0.03 ± 0.04* ($n = 10$)	8.80 ± 0.19* ($n = 10$)

n is the number of animals used to calculate the saliva flow rate. This table summarizes data previously reported in Xia *et al* (2003a), Shan *et al* (2005), and Li *et al* (2006).
*$P < 0.05$ compared with human using SPSS (11.5) statistical software.

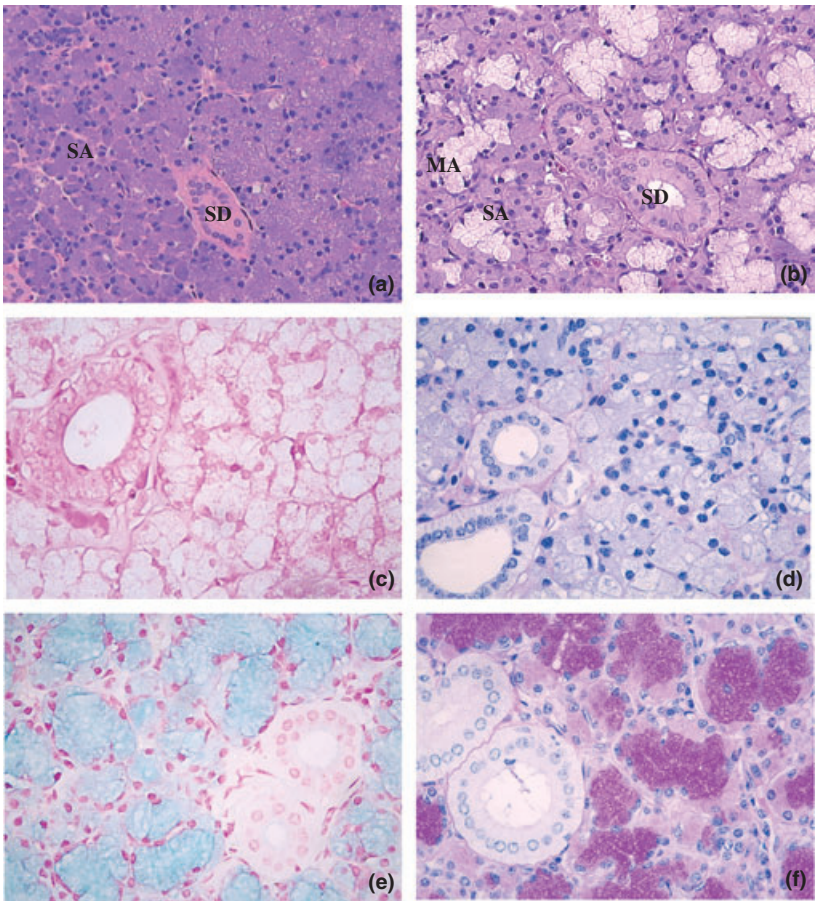

Figure 2 Hematoxylin and eosin (HE) histochemical staining results of parotid and submandibular glands of the miniature pig. (**a**) Photomicrograph of the parotid gland of the miniature pig stained with HE. The acinar cells of the terminal portion of the parotid gland are cuboidal or pyramidal in shape and share the general cytologic characteristics of a typical serous acinar cell (SA). This includes the spherical nucleus located near the base of the cell and a cytoplasm full of granules. SD shows striated duct of parotid glands (×200). (**b**) Photomicrograph of the submandibular gland of the miniature pig stained with HE showing a parenchyma of mixed acini (MA) and serous acini (SA). Mucous cells contain a prominent nucleus located at the base of each cell. The serous cells have large basal nuclei and vacuolated secretory granules. SD shows striated duct of submandibular glands (×200). (**c**) Photomicrograph of miniature pig's parotid gland stained with alcian blue (pH 2.5) – no alcian blue positive staining is found (×400). (**d**) Photomicrograph of miniature pig's parotid gland stained with periodic acid-Schiff – no purplish-red staining is found in parotid glands because of the absence of mucous acini (×400). (**e**) Photomicrograph of a tissue sample from the submandibular gland stained with alcian blue (pH 2.5). Blue staining in the majority of acinar cells indicates the existence of acid mucous substance (×400). (**f**) Photomicrograph of tissue sample from the submandibular gland stained with periodic acid-Schiff. Purplish-red staining in the majority of acinar cells indicates the existence of polysaccharide, neutral mucous substance, and zymogen (×400)

irradiation equal to conventional fractions. The parotid flow rates and gland weights significantly decreased in both the 15 and 20 Gy groups post-IR. In the 20 Gy group, salivary flow rates were reduced by approximately 80% at 16 weeks post-IR. The results suggested that a single dose of 20 Gy could establish a useful model of irradiation damage to parotid glands. Additionally, the acinar cell areas in both IR groups were greatly reduced, and structural changes in salivary gland parenchyma occurred relatively early after IR, whereas the alterations in salivary output were relatively delayed. Further, reductions in salivary flow were not propor-

tional to acinar cell area loss, and the function in the non-irradiated side of the gland also decreased. These findings suggest that non-parenchymal IR damage likely contributes to IR-induced salivary hypofunction.

Using the miniature pig model with irradiation-damaged parotid glands, Lotz investigated the effects of orciprenaline-carbachol on radioprotection of miniature pig salivary glands. The doses of X-irradiation were 36 Gy, given as 6×6 Gy in 3 weeks. The findings confirmed the radioprotective effect of pharmacologically induced degranulation of acinar cells (Lotz *et al*, 1990).

Gene transfer studies

Localized gene transfer to salivary glands has great potential for the treatment of salivary gland, systemic, and oral diseases (Baum *et al*, 2006). Previous results suggested that adenoviral (Ad)-mediated transfer of the human aquaporin-1 (hAQP1) cDNA, encoding a water channel protein, to rat submandibular glands following IR restored salivary flow to near-normal levels (Delporte *et al*, 1997). Our group transferred AdCMVluc, a recombinant type 5 adenoviral (rAd5) vector containing a luciferase reporter gene, and AdCMVlacZ, a similar rAd5 vector encoding β-galactosidase, to miniature pig parotid glands by intraductal cannulation (Li *et al*, 2004). The transgene expression by, and inflammatory response to, rAd5 vectors in miniature pig parotid glands were similar to results seen earlier in rodent studies. The AdhAQP1 construct was then transferred after parotid gland IR (20 Gy) in the miniature pig, Salivation from the targeted gland had decreased by $>80\%$ 16 weeks after IR. AdhAQP1 administration resulted in a dose-dependent increase in parotid salivary flow to approximately 80% of pre-IR levels on day 3 (Shan *et al*, 2005). The effective AdhAQP1 dose was 2.5×10^5 plaque-forming units (PFU) μl^{-1} infusate, a dose that leads to comparable transgene expression in murine and miniature pig salivary glands. Three days after Ad vector administration, little change was observed in clinical chemistry and hematology values. These findings demonstrate that localized delivery of AdhAQP1 to IR-damaged salivary glands increases salivary secretion, without significant general adverse events, in a large animal model. The results provided excellent preclinical evidence in support of developing a clinical trial to test whether the hAQP1 cDNA transfer strategy will be clinically effective in restoring salivary flow in patients with IR-induced parotid hypofunction.

Tooth and bone research

Anatomy and structure

The miniature pig has both deciduous and permanent dentitions. The initiation of tooth development and eruption in the miniature pig is quite similar to that in humans. The dental formula of the deciduous dentition for the miniature pig is Di3/3, Dc1/1, Dp1/1, Dm3/3 (Weaver *et al*, 1966), or Di3/3,Dc1/1,Dp2/3,Dm2/1 (Table 3, Figure 3a,b) (Li, 1993); for the permanent dentition it is I3, C1, P4 (3), M3 (maxillary) and I3, C1, P3 (4), M3 (mandible) (Figure 3c,d). The brackets indicate differences reported. The number of premolars usually stated for pigs is four in each quadrant, the same as for primitive mammals. However, the first of these is a small, variable tooth that if present, may be a retained deciduous tooth with or without a permanent successor. In general, the miniature pig has 32 deciduous and 44 permanent teeth, i.e., 12 more of each type than occur in humans. The sequence of eruption of permanent teeth is M1, C, I3, M2, P3, P4, I1, P2, I2, M3 (maxillary) and M1, I3, C, M2, I1, P4, P3, P2, I2, M3 (mandible) (Weaver *et al*, 1969). The third deciduous incisor and cuspid erupt by birth in the miniature pig, and all deciduous teeth erupt completely in the following 6–8 months. The permanent teeth erupt from 4 to 24 months after birth. There are some similarities in comparisons and correlations between the eruption times and sequence of miniature pig teeth with human teeth. These include the eruption of the first molar as the first permanent tooth to appear, the long period of mixed dentition that follows before the deciduous teeth are all replaced, and the apparent association of tooth eruption time and sequence with the sex of the individual. The teeth that are most variable and have the longest range of eruption times include incisors and third molars of both humans and miniature pigs.

Table 3 The eruption time of deciduous and permanent teeth in the miniature pig

Deciduous teeth	*Age at eruption*	*Permanent teeth*	*Age at eruption (months)*
Di1	1–3 weeks	I1	12–16
Di2	2–3 months	I2	16–20
Di3	Before birth	I3	8–10
Dc	Before birth	C	8–10
Dp1	6–8 months	P1(mandible)	18–24
Dp2	1–2.5 months	P1(maxillary)	>28
Dm1	1–5 weeks	P2, P3, P4	12–15
Dp3			
Dm2	1.5–2 months	M1	4–6
Dm		M2	9–12
		M3	24–28

This table summarizes data previously reported in Li (1993).

The size and morphology of the miniature pig's deciduous teeth are similar to humans. However, almost all the permanent teeth in the miniature pig are larger than in humans. All anterior teeth in the miniature pig have a very short crown and a long simple root, and the length of the root is two to three times than that of the crown (Li, 1993). The long axis of mandibular anterior teeth is inclined 30° to the occlusal surface. The cuspids are the most specialized teeth in the miniature pig. The upper cuspid is cone-shaped, and the root is very strong and directed distally. The lower cuspid is crook-shaped, and the root is curved distally. Generally, most premolars of the miniature pig have a wedge-shaped crown with a mesial-to-distal cutting-edge margin and mesial and distal roots. However, the morphology of the maxillary fourth premolar is similar to that of the human premolar and has two cusps, buccal and lingual,

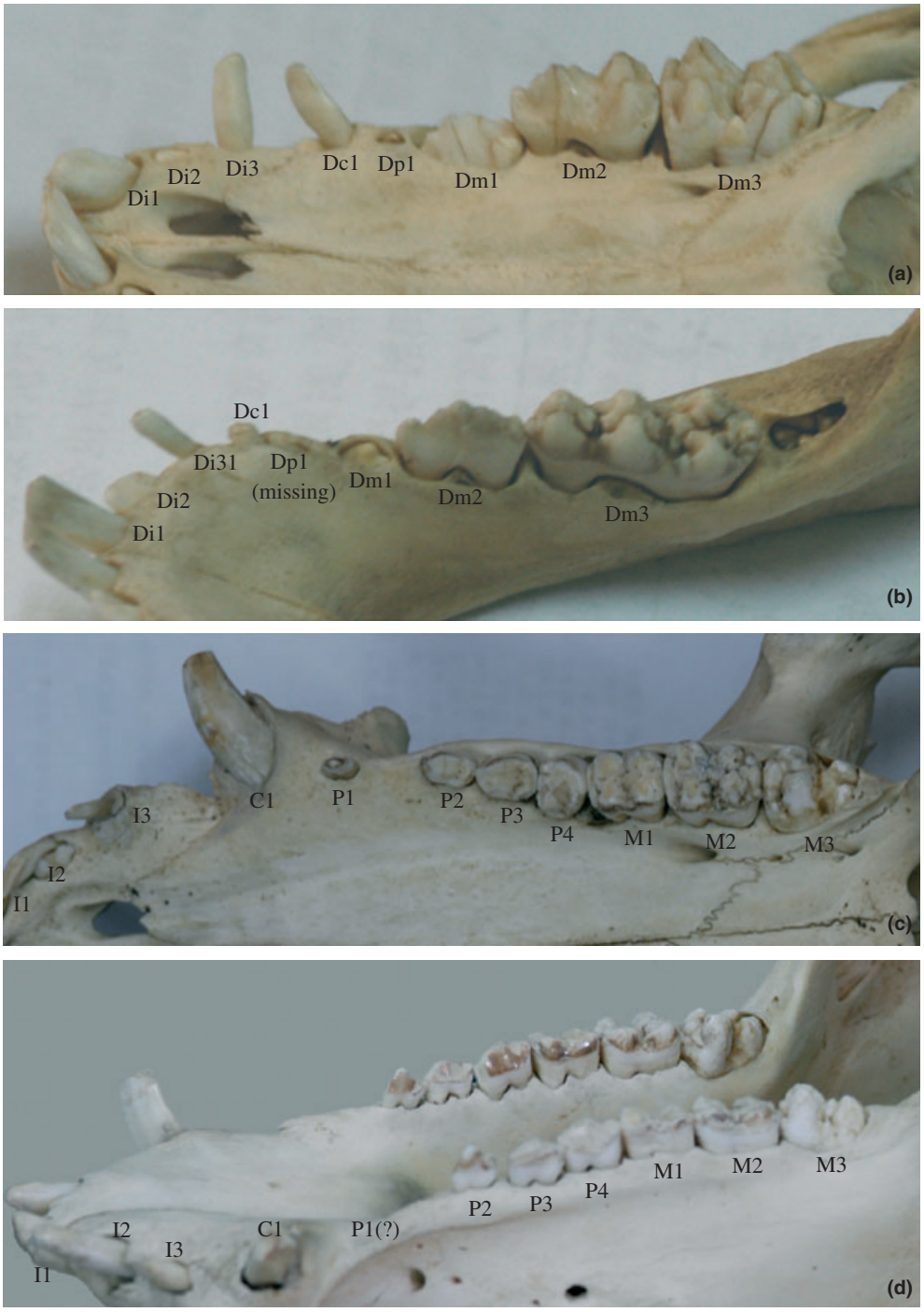

Figure 3 Deciduous and permanent dentitions of miniature pig. (**a**) Photograph showing deciduous dentition of maxillary of miniature pig at the age of 2 months: Di3, Dc1, Dp1, Dm3. (**b**) Photograph showing deciduous dentition of mandible of miniature pig at the age of 2 months: Di3, Dc1, Dp1, Dm3 (Dp1 missing). (**c**) Photograph showing permanent dentition of maxillary of miniature pig at the age of 24 months: I3, C1, P4 (3), M3. (**d**) Photograph showing permanent dentition of mandible of miniature pig at the age of 24 months: I3, C1, P3 (4), M3

and the maxillary third and fourth premolars have three to four roots. Miniature pig molars are larger, and have four to six roots. There are many grooves, fossae, and eminences on the occlusal surface. The maxillary molar is square-shaped and has four main cusps. The mandibular molar is oblong-shaped and has five to six main cusps.

The sulcular epithelium in the miniature pig consists of multi-layered squamous epithelium and lamina propria of the underlying connective tissue, and covers half of the crown (Meng *et al*, 1997). The depth of the gingival sulcus is 2–3 mm. The junctional epithelium is long and includes layers of flat cells paralleling the crown. Epithelial pegs and dermal papillae are long and slender

in free gingiva and short and blunt in the sulcular epithelium. The width of attached gingiva is similar to that in humans. In the miniature pig before 6 months of age little food debris or dental calculus can be found.

Periodontal diseases

Gingivitis often presents in the miniature pig after the age of 6 months. Swollen gingivae, accumulated plaque and calculus, a 1- to 2-mm red, flared zone on the gingival margin and bleeding on probing is frequently observed. There is infiltration of inflammatory cells, and blood vessels are edematous in the gingival tissues. Histologically, the inflammatory process is similar to that seen in human periodontal diseases. Serious periodontitis can be found in the miniature pig after the age of 16 months. The periodontal pocket depth (PD) may be up to 4–5 mm. Crestal resorption of the alveolar bone begins with the destruction of supporting bones.

Using ligatures, in association with bacteria, including *Porphyromonas gingivalis* (*Pg*), *Streptococcus mutans* (*Sm*), and *Actinobacillus actinomycetemcomitans* (*Aa*), can induce periodontitis in the Chinese miniature pig (Meng *et al*, 1996). At weeks 4 and 8, there are significant increases in mean probing depth (PD) values and clinical attachment loss (CAL). After this active phase, there is no further destruction up to 20 weeks. Following ligature removal, PDs decreased in 3 weeks, but never returned to the original baseline values.

Lang *et al* (1998) induced the bone defects in the furcation and interdental regions in miniature pigs and investigated the ability of the replanted cultured cells from alveolar bone and periodontal ligament to form new periodontal tissues. The results showed that defects healed largely by epithelialization without the replanted cells, and that replantation of cultured alveolar bone and periodontal ligament cells led to formation of new cementum and bone, which in turn led to formation of a new attachment. It was likely that the cells stabilized tissue formation in the defect or on the root surface in the early phase of wound healing and prevented epithelial downgrowth. Recent results also revealed that regeneration of the periodontium was determined by the availability of (precursor) cells capable of forming calcified tissues (Liu, Fang, Shi, Wang *et al*, unpublished data).

A similar method had been applied by Hickey *et al* (1991) to induce peri-implantitis in microswine. After ligation with silk suture material for a period of 45 days, the osseointegrated implants were susceptible to 'periodontal' breakdown or peri-implantitis. A greater CAL, increased PDs, and higher gingival index and plaque index scores were noted among the experimental implants. Radiographs revealed that experimental implants showed an increased amount of bone loss. The microbiota changed from primarily gram-positive facultative organisms to gram-negative obligate anaerobes, including black-pigmented *Bacteroides*, in experimental implants. Singh *et al* (1993) also induced peri-implantitis by the use of ligatures and a soft diet in the miniature pig. The surgical treatment effects of the guided tissue regeneration technique were evaluated by measuring osseous defects around the fixtures.

In summary, the miniature pig appears to be a suitable animal model for the evaluation of periodontal diseases and osseointegrated implants.

Tooth regeneration

Tooth tissue engineering is an emerging technique that may provide replacement teeth for patients suffering from diseases causing tooth loss. Although some attempts have been made to generate whole teeth both *in vivo* and *in vitro*, lack of knowledge about tooth initiation and development impede the progress of this technique. Mammalian tooth development is largely dependent on sequential and reciprocal epithelial–mesenchymal interactions. Further research is needed on the processes of epithelial–mesenchymal inductive interaction, the roles of multiple signaling molecules, and the links between different signaling loops. Seeking suitable cell resources for tooth regeneration, our group has cultured several stem cells by single-colony selection from adult miniature pigs *in vitro*, including dental pulp stem cells, periodontal stem cells, and bone marrow mesenchymal stem cells. These stem cells shared characteristics with similar human cells (Gronthos *et al*, 2002; Shi and Gronthos, 2003; Seo *et al*, 2004) and reacted positively to the antibody STRO-1, which recognizes primitive mesenchymal progenitor cells. These STRO-1-positive stem cells could differentiate into other types of cells *in vitro*, for example lipocyte. We isolated stem cells from apical papilla and periodontal ligament stem cells from the miniature pig and found that these cells generated a tooth/periodontal complex which could serve as a support for subsequent installation of a porcelain crown, leading to recovery of the tooth masticatory function and cosmetic appearance (Sonoyama, Liu, Fang, Yamaza, Seo, Zhang, He, Grathos, Wang, Swang, Shi, unpublished data).

Osteoradionecrosis

Although the anterior parts of the maxilla and mandible of the miniature pig are long, narrow, and protruding, the posterior part of the mandible, including the body of the mandible, ascending ramus, and temporal mandibular joint, is similar to human counterparts. Previous research on osteoradionecrosis (ORN) documented many disadvantages in the choices of experimental animals and the irradiation techniques (Schwartz and Kagan, 2002). Our group used three-dimensional conformal radiotherapy (3D-CRT), with a single dose of 25 Gy plus tooth extraction, to establish an ORN animal model in the mandible of the miniature pig. We reached a diagnosis of ORN by gross observations and the results of X-ray film, computerized tomography, scanning electron microscopy, and histopathologic examinations. These results suggested that the miniature pig mandible, subjected to a single 25-Gy dose of irradiation and tooth extraction, also may be a useful animal model of ORN (Fang, Sonoyama, Liu, Zhang, Yamaza, Shi, Wang, in preparation).

Other applications

Our group also observed the growth of miniature pig parotid cells on biomaterials *in vitro* for tissue engineering of artificial salivary gland, and showed that the acinar and non-acinar cells grow well and formed a monolayer on the biomaterials. The cultured miniature pig parotid gland cells remained polarized and secreted amylase *in vitro* (Sun *et al*, 2006). We also used this animal model to induce atrophy of the parotid glands in order to study the effect of these glands on body nitrate metabolism (Xia *et al*, 2003b). The miniature pig has also been used for testing implant materials and techniques (Schultze-Mosgau *et al*, 2000; Buchter *et al*, 2005; Nkenke *et al*, 2005), for reconstruction of craniofacial and temporal mandibular joint fractures (Bermejo *et al*, 1993; Niederhagen *et al*, 1999; Hollister *et al*, 2000; Wurzler *et al*, 2004), for studies on the biological properties of the periodontal tissues and the treatment of periodontal diseases (Kalkwarf and Krejci, 1983; Craig *et al*, 2004; Ziegler *et al*, 2005), and on the therapy of obstructive sleep apnea syndrome (Chen *et al*, 2000; Li *et al*, 2005a).

In conclusion, the miniature pig is increasingly used in many biomedical studies because of its similarity in gross anatomy and physiology to humans, as well as for other scientific, economic, and ethical reasons. We believe the miniature pig is a valuable preclinical animal model that can be widely used in oral and craniofacial research.

Acknowledgements

This work was partially supported by the National Natural Science Foundation of China (Grants 30125042, 30271400, 30430690, and 30428009), Beijing Scientific Grant 7002020, and Beijing Major Scientific Program grant (D0906007000091). The authors express sincere gratitude to Dr. Bruce Baum, NIDCR, NIH, USA, and Prof. Xiaomin Wang, Capital Medical University, China, for their encouragement and critical reading of this review.

References

Baum BJ, Zheng C, Cotrim AP *et al* (2006). Transfer of the AQP1 cDNA for the correction of radiation-induced salivary hypofunction. *Biochim Biophys Acta* **1758:** 1071–1077.

Bermejo A, Gonzalez O, Gonzalez JM (1993). The pig as an animal model for experimentation on the temporomandibular articular complex. *Oral Surg Oral Med Oral Pathol* **75:** 18–23.

Buchter A, Kleinheinz J, Wiesmann HP *et al* (2005). Biological and biomechanical evaluation of bone remodelling and implant stability after using an osteotome technique. *Clin Oral Implants Res* **16:** 1–8.

Chen L, Shi Q, Scharf SM (2000). Hemodynamic effects of periodic obstructive apneas in sedated pigs with congestive heart failure. *J Appl Physiol* **88:** 1051–1060.

Craig RG, Kallur SP, Inoue M, Rosenberg PA, LeGeros RZ (2004). Effect of enamel matrix proteins on the periodontal connective tissue-material interface after wound healing. *J Biomed Mater Res A* **69:** 180–187.

Delporte C, O'Connell BC, He X *et al* (1997). Increased fluid secretion after adenoviral-mediated transfer of the aquaporin-1 cDNA to irradiated rat salivary glands. *Proc Natl Acad Sci U S A* **94:** 3268–3273.

England DC, Winters LM, Carpenter LE (1954). The development of a breed of miniature swine; a preliminary report. *Growth* **18:** 207–214.

Gosselin TK, Pavilonis H (2002). Head and neck cancer: managing xerostomia and other treatment induced side effects. *ORL Head Neck Nurs* **20:** 15–22.

Gronthos S, Brahim J, Li W *et al* (2002). Stem cell properties of human dental pulp stem cells. *J Dent Res* **81:** 531–535.

Hickey JS, O'Neal RB, Scheidt MJ, Strong SL, Turgeon D, Van Dyke TE (1991). Microbiologic characterization of ligature-induced peri-implantitis in the microswine model. *J Periodontol* **62:** 548–553.

Hollister SJ, Levy RA, Chu TM, Halloran JW, Feinberg SE (2000). An image-based approach for designing and manufacturing craniofacial scaffolds. *Int J Oral Maxillofac Surg* **29:** 66–67.

Kalkwarf KL, Krejci RF (1983). Effect of inflammation on periodontal attachment levels in miniature swine with mucogingival defects. *J Periodontol* **54:** 361–364.

Lang H, Schuler N, Nolden R (1998). Attachment formation following replantation of cultured cells into periodontal defects – a study in minipigs. *J Dent Res* **77:** 393–405.

Larsen MO, Rolin B (2004). Use of the Gottingen minipig as a model of diabetes, with special focus on type 1 diabetes research. *ILAR J* **45:** 303–313.

Li YJ (1993). The characters of the dental system in Chinese minipig. *Zhonghua Kou Qiang Yi Xue Za Zhi* **28:** 234–236 (in Chinese).

Li J, Zheng C, Zhang X *et al* (2004). Developing a convenient large animal model for gene transfer to salivary glands in vivo. *J Gene Med* **6:** 55–63.

Li B, Zhao LM, Xiu QY *et al* (2005a). An experimental study on the minipig model of obstructive sleep apnea syndrome. *J Biomed Eng* **22:** 565–569 (in Chinese).

Li J, Shan Z, Ou G *et al* (2005b). Structural and functional characteristics of irradiation damage to parotid glands in the miniature pig. *Int J Radiat Oncol Biol Phys* **62:** 1510–1516.

Li YT, Liu Y, Zhang CM, Liu XY, Wang SL (2006). Comparative analysis of mixed saliva flow rate, pH, buffer capacity and biochemistry among miniature pigs, rats and humans. *Beijing J Stomatol* (in press) (in Chinese).

Lotz S, Caselitz J, Tschakert H, Rehpenning W, Seifert G (1990). Radioprotection of minipig salivary glands by orciprenaline-carbachol. An ultrastructural and semiquantitative light microscopic study. *Virchows Arch A Pathol Anat Histopathol* **417:** 119–128.

Ma DQ (2002). *Diseases of the salivary glands*, 2nd edn. People's Health Publishing House: Beijing (in Chinese).

Meng H, Xie H, Chen Z (1996). Evaluation of ligature-induced periodontitis in minipig. *Zhonghua Kou Qiang Yi Xue Za Zhi* **31:** 333–336 (in Chinese).

Meng H, Cao C, Zhang SW, Chen ZB, Zhang KH, Wang HJ (1997). The study of gingivitis in deciduous teeth of minipigs. *J Beijing Med Univ* **29:** 53–55 (in Chinese).

Millikan LE, Boylon JL, Hook RR, Manning PJ (1974). Melanoma in Sinclair swine: a new animal model. *J Invest Dermatol* **62:** 20–30.

Nagler RM (2003). Effects of head and neck radiotherapy on major salivary glands – animal studies and human implications. *In Vitro* **17:** 369–375.

Niederhagen B, Braumann B, Schmolke C, Appel T, von Lindern JJ, Berge S (1999). Tooth-borne distraction of the mandible. An experimental study. *Int J Oral Maxillofac Surg* **28:** 475–479.

Nkenke E, Lehner B, Fenner M *et al* (2005). Immediate versus delayed loading of dental implants in the maxillae of minipigs: follow-up of implant stability and implant failures. *Int J Oral Maxillofac Implants* **20:** 39–47.

Polejaeva IA, Chen SH, Vaught TD *et al* (2000). Cloned pigs produced by nuclear transfer from adult somatic cells. *Nature* **407:** 86–90.

Radfar L, Sirois DA (2003). Structural and functional injury in minipig salivary glands following fractionated exposure to 70 Gy of ionizing radiation: an animal model for human radiation-induced salivary gland injury. *Oral Surg Oral Med Oral Pathol Oral Radiol Endod* **96:** 267–274.

Schultze-Mosgau S, Schliephake H, Radespiel-Troger M, Neukam FW (2000). Osseointegration of endodontic endosseous cones: zirconium oxide vs titanurm. *Oral Surg Oral Med Ord Pathol Oral Radiol Endod* **89:** 91–98.

Schwartz HC, Kagan AR (2002). Osteoradionecrosis of the mandible: scientific basis for clinical staging. *Am J Clin Oncol* **25:** 168–171.

Screaton NJ, Coxson HO, Kalloger SE *et al* (2003). Detection of lung perfusion abnormalities using computed tomography in a porcine model of pulmonary embolism. *J Thorac Imaging* **18:** 14–20.

Seo BM, Miura M, Gronthos S *et al* (2004). Multipotent postnatal stem cells from human periodontal ligament. *Lancet* **364:** 149–155.

Shan Z, Li J, Zheng C *et al* (2005). Increased fluid secretion after adenoviral-mediated transfer of the human aquaporin-1 cDNA to irradiated miniature pig parotid glands. *Mol Ther* **11:** 444–451.

Shi S, Gronthos S (2003). Perivascular niche of postnatal mesenchymal stem cells in human bone marrow and dental pulp. *J Bone Miner Res* **18:** 696–704.

Singh G, O'Neal RB, Brennan WA, Strong SL, Horner JA, Van Dyke TE (1993). Surgical treatment of induced periimplantitis in the micro pig: clinical and histological analysis. *J Periodontol* **64:** 984–989.

Sun T, Zhu J, Yang X, Wang SL (2006). Growth of miniature pig parotid cells on biomaterials in vitro. *Arch Oral Biol* **51:** 351–358.

Van Dorp AG, Verhoeven MC, Koerten HK, Van Der Nat-Van Der Meij TH, Van Blitterswijk CA, Ponec M (1998). Dermal regeneration in full-thickness wounds in Yucatan miniature pigs using a biodegradable copolymer. *Wound Repair Regen* **6:** 556–568.

Wang SL, Li J, Zhu XZ, Sun K, Liu XY, Zhang YG (1998). Sialographic characterization of the normal parotid gland of the miniature pig. *Dentomaxillofac Radiol* **27:** 178–181.

Weaver ME, Jump EB, McKean CF (1966). The eruption pattern of deciduous teeth in miniature swine. *Anat Rec* **154:** 81–86.

Weaver ME, Jump EB, McKean CF (1969). The eruption pattern of permanent teeth in miniature swine. *Arch Oral Biol* **14:** 323–331.

Wurzler KK, Heisterkamp M, Bohm H, Kubler NR, Sebald W, Reuther JF (2004). Mandibular reconstruction with autologous bone and osseoinductive implant in the Gottingen minipig. *Mund Kiefer Gesichtschir* **8:** 75–82.

Xia DS, Deng DJ, Wang SL (2003a). Alterations of nitrate and nitrite content in saliva, serum, and urine in patients with salivary dysfunction. *J Oral Pathol Med* **32:** 95–99.

Xia DS, Deng DJ, Wang SL (2003b). Destruction of parotid glands affects nitrate and nitrite metabolism. *J Dent Res* **82:** 101–105.

Xu Q, Yu D, Qiu Y, Zhang H, Ding Y (2003). Function of a new internal bioartificial liver: an in vitro study. *Ann Clin Lab Sci* **33:** 306–312.

Yu SM, Wang CW, Zhao DM, Zhang QC, Pei DZ (2003). Raising and pathogen purification of Chinese experimental mini-pig. *Lab Anim Sci Admin* **20:** 44–46.

Zhang X, Li J, Liu XY, Sun YL, Zhang CM, Wang SL (2003). Comparative study of sialography and anatomy of salivary glands of five species experimental animals. *Beijing J Stomatol* **11:** 195–199 (in Chinese).

Zhang X, Li J, Liu XY, Sun YL, Zhang CM, Wang SL (2005). Morphological characteristics of submandibular gland of miniature pig. *Chin Med J* **118:** 1368–1373.

Ziegler A, Keilig L, Kawarizadeh A, Jager A, Bourauel C (2005). Numerical simulation of the biomechanical behaviour of multi-rooted teeth. *Eur J Orthod* **27:** 333–339.